GEOPHYSICAL RESEARCH LETTERS, VOL. 33, L13603, doi:10.1029/2006GL026155, 2006

Poleward propagation of spiciness anomalies in the North Atlantic Ocean

Audine Laurian,[1] Alban Lazar,[1] Gilles Reverdin,[1] Keith Rodgers,[1] and Pascal Terray[1]

Received 27 February 2006; revised 19 May 2006; accepted 30 May 2006; published 6 July 2006.

[1] Recent modelling results suggest that subsurface salinity anomalies propagating from the tropics can reach and precondition the deep-water formation regions, thus modulating the THC variability. The forcing and propagative aspects of this mechanism are presented in the North Atlantic Ocean over 1948–2002 using an OGCM. Density compensated salinity anomalies of 0.1 up to 0.35 psu along σ = 26 kg.m^{-3} are generated in the salinity maximum region at interannual to decadal frequency. The relation between subsurface conditions and late winter sea surface salinity variability supports the subduction mechanism. They circulate over isopycnals ranging from 25.6σ to 26.2σ at current speed between 150 m and 250 m depth toward Cape Hatteras via the Gulf of Mexico on a typical 6-year transit. Although mixing along the pathway reduces the amplitude of salinity anomalies by about 66%, they largely determine the subsurface spiciness of the Gulf Stream up to 30°N, upstream of the outcrop region. **Citation:** Laurian, A., A. Lazar, G. Reverdin, K. Rodgers, and P. Terray (2006), Poleward propagation of spiciness anomalies in the North Atlantic Ocean, *Geophys. Res. Lett.*, *33*, L13603, doi:10.1029/2006GL026155.

1. Introduction

[2] The upper branch of the thermohaline circulation (THC) plays an important role in global climate variability by transporting large amounts of heat and salt poleward. The regions of deep convection and the THC may be affected by the temperature and salinity trends observed in the North Atlantic Ocean (NATL) during the last 50 years [*Curry et al.*, 2003; *Boyer et al.*, 2005; *Vellinga and Wu*, 2004]. While most coupled models [*Manabe and Stouffer*, 1993; *Stocker and Schmittner*, 1997; *Häkkinen*, 1999] suggest a weakening of the THC in response to global warming and freshening at high latitudes, *Latif et al.* [2000] among others suggest that poleward advection of tropical waters with anomalously high salinity could compensate global warming effects by stabilizing the THC. In the NATL, the salinity maximum water (SMW) region is a main region for the renewal of the subtropical gyre thermocline waters and large volumes of anomalously salty waters can be produced there by ventilation [*Blanke et al.*, 2002; *Lazar et al.*, 2002]. According to *Thorpe et al.* [2001], the advection of salinity anomalies from low to high latitudes is achieved at subsurface with a time scale of 5–6 decades [*Vellinga and Wu*, 2004]. This might be related to the propagation of subsurface density-compensated salinity anomalies (CSAs) studied on interannual timescale. Along with their associated temperature anomalies (CTAs) they have been shown to propagate on isopycnal surfaces at current speed in the Pacific Ocean [*Schneider*, 2000; *Nonaka and Xie*, 2000; *Yeager and Large*, 2004; *Luo et al.*, 2005] and in the South Atlantic Ocean [*Lazar et al.*, 2001]. We describe and analyse the propagation of the CSAs in the NATL and examine their relation to the surface signals with a 55-years simulation from an OGCM.

2. Model and Simulation

[3] We use monthly mean outputs from the OPA version 8.1 OGCM [*Madec et al.*, 1998]. The zonal resolution is 2°, the meridional resolution is 2° × cos(latitude), increasing to 1/3° at the equator and there are 31 vertical levels with variable thickness. The model uses the *Gent and McWilliams* [1990] eddy parameterization scheme poleward of 20°, and the turbulent kinetic energy scheme of *Blanke and Delecluse* [1993] is used for vertical mixing. Surface heat fluxes are calculated using bulk formulas based on daily mean NCEP reanalyses over 1948–2002, and the surface boundary condition for freshwater fluxes is a relaxation of salinity to annual mean values from the *Boyer et al.* [1998] climatology with restoring time of 12 days.

[4] Supposing that the CSAs are forced by the surface, we examine the mixed layer depth (MLD) cycle and the SMW distribution. The maximum MLD in the subtropical gyre occurs in late January–early March (not shown) in agreement with observations [e.g., *de Boyer Montégut et al.*, 2004]; the CSAs are generated during this period. The simulated February mean position of the SMW region is shifted eastward by 10° relative to the observations (Figure 1) due to a bias in the NCEP reanalysis products of wind speed and precipitation. As a consequence, surfaces of higher density than in the observations outcrop in the SMW region (26 to 26.5σ vs. 25.5 to 26σ; $\sigma = \rho - 1000$, ρ is the potential density in kg.m^{-3}, not shown). Given this geographical shift, the formation and propagation mechanisms should occur on slightly different layers.

3. Analysis Methodology

[5] To analyse and follow CSAs along their pathway, we project the salinity field onto time-varying potential density surfaces, referenced to the surface pressure. A CSA is defined as the difference between the salinity on the isopycnal, S_σ and its monthly climatology $\overline{S_\sigma}$ over 1948–2002 (idem for CTA).

[1]Laboratoire d'Océanographie et du Climat: Expérimentation et Approche Numérique, Institut Pierre Simon Laplace, Paris, France.

0094-8276/06/2006GL026155$05.00

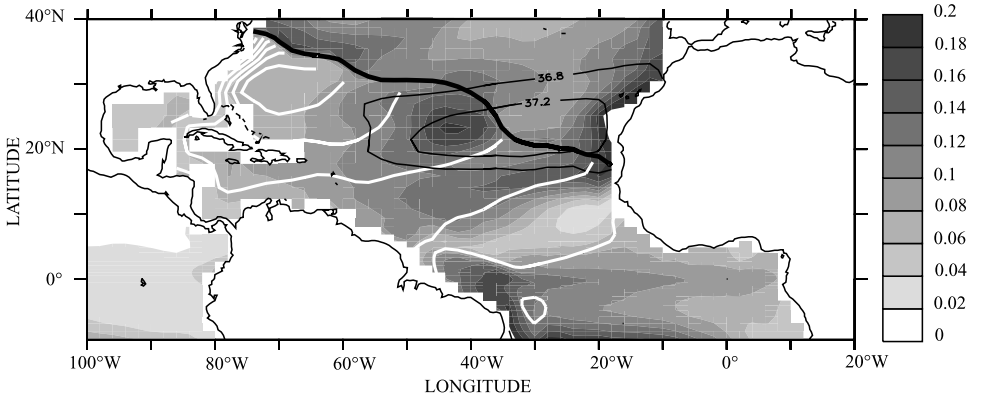

Figure 1. Rms CSAs on 26σ and rms SSSAs north of the winter mean outcrop line (bold black contour) from 1948–2002. Winter mean isolines of Bernoulli function (considering monthly means of ρ, u and v over 1948–2002) are contoured in white and the annual mean isolines of SSS are also shown.

[6] In order to track these subsurface anomalies, we need a time integrated view of their circulation. Thermocline pathways can be described assuming that turbulent mixing is sufficiently weak (true away from the surface, upwelling regions and boundaries) so that waters conserve their density and Bernoulli function (B). Under this hypothesis, fluid trajectories can be approximated by the isopycnal projection of interannual B, defined as:

$$B(\sigma_0) = \frac{\rho_0}{2}\left(u^2 + v^2\right) + \rho_0 g\eta + g\int_{z(\sigma_0)}^{0} [\sigma(z) - \sigma_0]dz$$

where σ, u, v and η are interannual values of potential density, horizontal velocity components, and sea surface elevation. As shown later, the downstream tracking of CSAs can be achieved by plotting x-y averages of CSAs within a given pathway of interannual B following *Lazar et al.* [2001].

4. Results

[7] The spatial distribution and amplitude of CSAs generated in the SMW region is highlighted by their root mean square (rms) over 1948–2002 and displayed on Figure 1. A dipole south of the winter mean 26σ outcrop line between 41°W–23°N and 20°W–16°N is composed of two regions of high CSA rms (.2 psu; rms of associated CTAs is about .45°C, not shown) situated northwest and southeast of the SMW region. The amplitude of CSAs is of the same order of magnitude as what was found in previous studies [*Schneider*, 2000; *Yeager and Large*, 2004] and it is reduced by about 66% along the interannual pathway most likely due to diabatic processes. Note the strong CSA rms (.18) along the equator corresponds to the signals described by *Lazar et al.* [2001]. The late winter sea surface salinity anomalies (SSSAs) rms north of the winter mean 26σ outcrop line highlights a dipole as well. The regions of strong SSSAs rms are collocated with regions of strong SSS gradients (not shown) where current anomalies will have the strongest impacts thus favouring advective processes rather than atmospheric processes to account for the generation of CSAs. Note the maximum of variance of SSSAs in the Gulf Stream can be explained by this mechanism. The collocation between the dipoles of CSA rms and SSSA rms, which are persistent structures, strongly supports our hypothesis of surface generation of the CSAs.

[8] We estimate the timescale of the propagation of these CSAs with lagged correlations (Figure 2). The reference

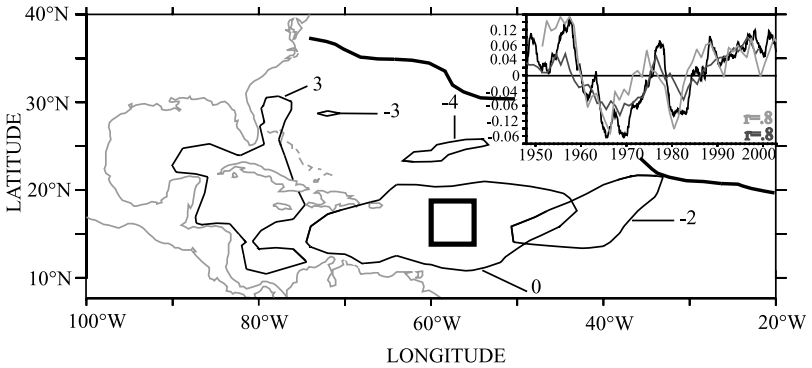

Figure 2. Correlations higher than 0.8 between monthly CSAs on 26σ and monthly CSAs on 26σ averaged in the index zone (black rectangle and black time series) are shown for lags −4, −3, −2, 0 and 3 year. The dark grey time series is annual CSAs averaged in 80°W–78°W, 30°N with a 3-year negative lag and the light grey time series is late winter SSSAs averaged in 20°W–30°W, 22°N–28°N with a 3-year positive lag. The winter mean outcrop line of 26σ is shown.

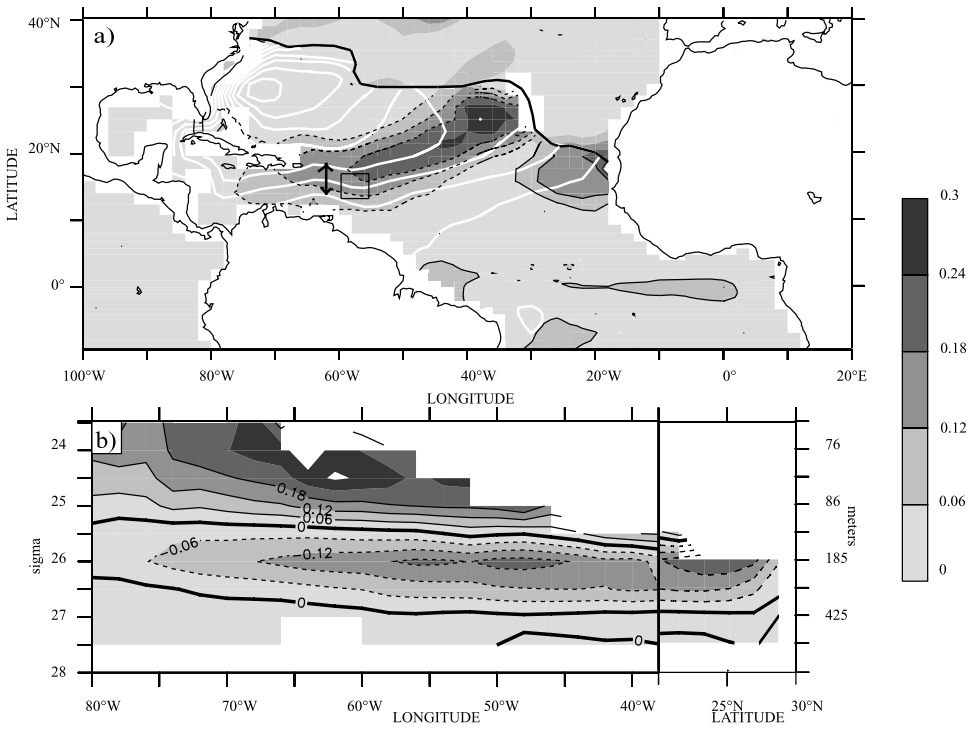

Figure 3. (a) CSAs along the 26σ and SSSAs in February 1980. The winter mean isolines of B (white contours), the outcrop region of 26σ in February 1980 and the index zone are also shown. The tracking of CSAs is achieved by plotting x-y averages of CSAs within the two isolines of B delimited by the arrow. (b) Salinity anomalies averaged in longitude north of 20°N and in latitude south of 20°N between the two isolines of B noted by the arrow on Figure 3a from the SMW region to the Yucatan Strait in February 1980 are contoured (potential density as vertical left axis, mean depth in meter as right axis).

time series corresponds to monthly CSAs along 26σ over 1948–2002 averaged in 55–60°W, 13–18°N. This box is selected to retain only the CSAs entering the Caribbean Sea since they have the greatest potential to modulate the salinity field at high latitudes in a 5 to 10 years timescale (CSAs flowing north of the Caribbean tend to recirculate and reach high latitudes on a longer time scale) [*Blanke et al.*, 2002]. We correlate the monthly CSAs along 26σ with this time series. The amplitude of these CSAs is in the range ±0.15 and they propagate as a coherent signal over 6 years following the thermocline advective pathways, from the winter outcrop line of 26σ to 30°N in the Gulf Stream. This time series and the time series of late winter SSSAs averaged in the SMW region (20°W–30°W, 22°N–28°N) lagged by 3 years are highly correlated (r = .8), a result which supports further a generation mechanism by surface processes. These results hold for isopycnals ranging from 25.0 to 26.5 (not shown). Although correlations are not significant downstream of this region after a 3-year lag and despite a decrease of about 66% of the amplitude of the CSAs (compare time series in Figure 2), the regression of the time series of monthly CSAs in the SMW region (20°W–30°W, 22°N–28°N) by the time series of monthly CSAs in the Gulf Stream (80°W–78°W, 30°N) with a 5 year lag explains nearly 70% of the variance of CSAs in the Gulf Stream.

[9] To display the horizontal and vertical patterns of 26σ CSAs, we show them in February 1980 when strong signals emanating from the dipole described above prevail (Figure 3). The horizontal structure (Figure 3a) displays two anomalies extending in the direction of the currents. A negative one (about −0.3 psu) has been created in the western SMW region, part of it extends toward the north of the Caribbean and part of it toward the Gulf of Mexico, and a positive one (about 0.2) has been created in the east of the SMW region. This structure is quite common from 1948–2002. The mixing between positive and negative CSAs of the dipole favours the damping of the signal and may explain the low rms of CSAs entering the Caribbean Sea (Figure 1). The vertical structure of the CSAs described above from the permanent thermocline in the SMW region to the Yucatan Strait and averaged in latitude between the two isolines of B noted by the arrow on Figure 3a is presented on Figure 3b. The core of the negative CSA (−0.18 psu) centered on 26σ extends from 25.5σ to 26.8σ (vertical extension of about 90m). A large positive CSA (0.3) extends from 23.5σ to 25σ (vertical extension of about 15m). Again, the two opposite signals favour and increase the damping. The strong vertical gradients (about 2.10^{-3} psu.m^{-1}) might strengthen double diffusion which damps the CSAs in the real ocean although in the Pacific *Yeager and Large* [2004] showed that salt fingering has little effect on the variability of isopycnal salinity.

[10] To document the interannual variability of the creation and propagation of CSAs, a Hovmöller diagram of monthly 26σ CSAs along their pathway (averaged between the isolines of B noted by the arrow on Figure 3a) is presented on Figure 4 as well as the time series of late winter SSSAs averaged in 20°W–30°W, 22°N–28°N. As was said before, the time series (Figure 4a) strongly

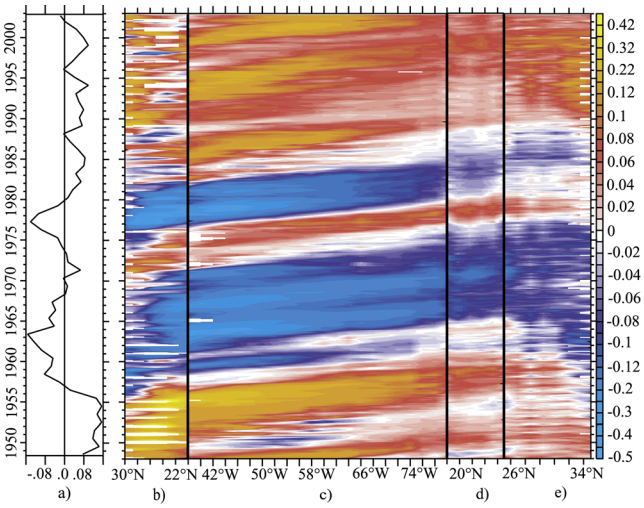

Figure 4. (a) Time series of late winter SSSAs in the formation region (20°W–30°W, 22°N–28°N). (b–e) Hovmöller diagrams of the monthly CSAs on 26σ along the pathway. Outcrop region in the SMW (Figure 4b), from the SMW to the Gulf of Mexico (Figure 4c), Gulf of Mexico (Figure 4d), and from Florida to Cape Hatteras (Figure 4e). (The color palette is non linear.)

supports a subduction mechanism for the generation of CSAs. Moreover, sign-liked CSAs are generated during successive years. For instance, positive CSAs were created from 1948 to 1955 and propagated via the Gulf of Mexico (Figure 4b–4d) toward Cape Hatteras (Figure 4e) in about 6 years with an amplitude decreasing from .15 to .05 (corresponding to .6 to .1°C) along their way. From 1955 to 1966, negative CSAs were injected in the thermocline and propagated in 6–8 years with an amplitude decreasing from −.2 to −.06 (−.4 to −.2°C) along the same pathway. The amplitude of the signals decreases due to mixing all along the pathway. This mixing may be amplified by the horizontal and vertical dipoles described above. Another mechanism alters the amplitude of the CSAs: for instance the positive anomalies reaching the vicinity of Cape Hatteras (Figure 4e) between 1990 and 2000 have stronger amplitude than they did when they were generated (Figure 4b). A possible explanation is the mixing along 26σ of these CSAs with stronger positive anomalies that drifted north of the Caribbean Islands reaching the same region or the mixing of these CSAs with stronger signals on lighter isopycnals. This alteration of amplitude remains an open question. Despite these reductions in amplitude, about 34% of the signal remains identifiable until Cape Hatteras (Figure 4e). The propagation speed of these anomalies between the SMW region and the Yucatan Strait (Figure 4b–4c) is about 2cm.s^{-1}, it increases to about 1m.s^{-1} in the Gulf of Mexico (Figure 4d) and in the Gulf Stream (Figure 4e), in agreement with measurements of current speed in these regions.

5. Discussion

[11] We analysed the propagation of CSAs generated in the SMW region of the North Atlantic Ocean toward Cape Hatteras from 1948 to 2002 in a global OGCM. The largest CSAs (0.1 up to 0.35 psu with associated temperature anomalies of 0.3 up to 0.6°C) are seen to propagate via the Gulf of Mexico along 26σ at current speed on a typical 6-year transit. The low-frequency of the signal appears to be forced by late winter SSSAs. Although mixing along the pathway reduces by about 66% the amplitude of the CSAs, they determine to a large extent (nearly 70%) the subsurface spiciness of the Gulf Stream water up to 30°N, upstream of the outcrop region. This propagation process analysis provides support to recent studies suggesting that the present pathway can be a key route for salinity perturbation toward the subpolar gyre, eventually modifying density, the THC and the sea level [*Latif et al.*, 2000; *Vellinga et al.*, 2004; *Levitus et al.*, 2005].

[12] High latitude impacts of these propagating anomalies involve several processes. First, mixing along the 6-year journey reduces the CSAs by 66%. It is possible though that the mixing is not well enough simulated and comparison with observations will be needed. Then one can expect the emergence and consequent mixing over the mixed layer (which annual mean depth in the Gulf Stream is only about 80 m) to further reduce their amplitude and generate a weaker compensated SSSA. At this stage atmospheric heat flux feedback may start to act and a model allowing coupled air-sea interactions would be needed. In the case of a spicy anomaly with positive SSSA and SST anomalies, the turbulent heat flux damping cools down the signal. Following *Frankignoul et al.* [1997], a SST anomaly of 0.2°C (typical amplitude observed below the mixed layer) should dissipate over 3 months (simultaneously creating, via the SST-evaporation feedback, a positive SSSA small compared to the compensated SSS signal of 0.1). During this decompensation period, where the SSTA weakens but not the SSSA, there is a positive surface density anomaly. Although this process implies weak densification, it should have more impact at decadal and longer timescales [*Schneider*, 2004] if long-lasting like-signed spiciness anomalies are injected in the source region.

[13] **Acknowledgment.** We thank R. Tailleux and two reviewers for very constructive comments. This work is supported by a PNEDC grant.

References

Blanke, B., and P. Delecluse (1993), Variability of the tropical Atlantic ocean simulated by a general circulation model with two different mixed layer physics, *J. Phys. Oceanogr.*, *27*, 1038–1053.

Blanke, B., M. Arhan, A. Lazar, and G. Prévost (2002), A Lagrangian numerical investigation of the origins and fates of the salinity maximum water in the Atlantic, *J. Geophys. Res.*, *107*(C10), 3163, doi:10.1029/2002JC001318.

Boyer, T. P., S. Levitus, J. Antonov, M. Conkright, T. O'Brien, and C. Stephens (1998), *World Ocean Atlas 1998*, vol. 5, *Salinity of the Pacific Ocean*, *NOAA Atlas NESDIS 30*, Silver Spring, Md.

Boyer, T. P., S. Levitus, J. I. Antonov, R. A. Locarnini, and H. E. Garcia (2005), Linear trends in salinity for the World Ocean, 1955–1998, *Geophys. Res. Lett.*, *32*, L01604, doi:10.1029/2004GL021791.

Curry, R., B. Dickson, and I. Yashayaev (2003), A change in the freshwater balance over the Atlantic Ocean over the past four decades, *Nature*, *426*, 826–829.

de Boyer Montégut, C., G. Madec, A. S. Fischer, A. Lazar, and D. Iudicone (2004), Mixed layer depth over the global ocean: An examination of profile data and a profile-based climatology, *J. Geophys. Res.*, *109*, C12003, doi:10.1029/2004JC002378.

Frankignoul, C., A. Czaja, and B. L'Heveder (1997), Air-sea feedback in the North Atlantic and surface boundary conditions for ocean models, *J. Clim.*, *11*, 2310–2324.

Gent, P. R., and J. C. McWilliams (1990), Isopycnal mixing in ocean circulation models, *J. Phys. Oceanogr.*, *20*, 150–156.

Häkkinen, S. (1999), A simulation of thermohaline effects of a great salinity anomaly, *J. Clim.*, *12*, 1781–1795.

Latif, M., E. Roeckner, U. Mikolajewicz, and R. Voss (2000), Tropical stabilization of the thermohaline circulation in a greenhouse warming simulation, *J. Clim.*, *13*, 1809–1813.

Lazar, A., R. Murtugudde, and A. J. Busalacchi (2001), A model study of temperature anomaly propagation from the subtropics to tropics within the South Atlantic thermocline, *Geophys. Res. Lett.*, *28*, 1271–1274.

Lazar, A., T. Inui, P. Malanotte-Rizzoli, A. J. Busalacchi, L. Wang, and R. Murtugudde (2002), Seasonality of the ventilation of the tropical Atlantic thermocline in an ocean general circulation model, *J. Geophys. Res.*, *107*(C8), 3104, doi:10.1029/2000JC000667.

Levitus, S., J. I. Antonov, T. P. Boyer, H. E. Garcia, and R. A. Locarnini (2005), Linear trends of zonally averaged thermosteric, halosteric, and total steric sea level for individual ocean basins and the world ocean, (1955–1959)–(1994–1998), *Geophys. Res. Lett.*, *32*, L16601, doi:10.1029/2005GL023761.

Luo, Y., L. M. Rothstein, R. Zhang, and A. J. Busalacchi (2005), On the connection between South Pacific subtropical spiciness anomalies and decadal equatorial variability in an ocean general circulation model, *J. Geophys. Res.*, *110*, C10002, doi:10.1029/2004JC002655.

Madec, G., P. Delecluse, M. Imbard, and C. Lévy (1998), OPA 8.1, Ocean general circulation model reference manual, *Note 11*, 91 pp., l'Institut Pierre Simon Laplace, Paris, France.

Manabe, S., and R. J. Stouffer (1993), Century-scale effects of increased atmospheric CO_2 on the ocean-atmosphere system, *Nature*, *364*, 215–218.

Nonaka, M., and S. P. Xie (2000), Propagation of North Pacific interdecadal subsurface temperature anomalies in an ocean GCM, *Geophys. Res. Lett.*, *27*, 3747–3750.

Schneider, N. (2000), A decadal spiciness mode in the tropics, *Geophys. Res. Lett.*, *27*, 257–260.

Schneider, N. (2004), The response of tropical climate to the equatorial emergence of spiciness anomalies, *J. Clim.*, *17*, 1083–1095.

Stocker, T. F., and A. Schmittner (1997), Influence of CO2 emission rates on the stability of the thermohaline circulation, *Nature*, *388*, 862–865.

Thorpe, R. B., J. M. Gregory, T. C. Johns, R. A. Wood, and J. F. B. Mitchell (2001), Mechanisms determinig the Atlantic thermohaline circulation response to greenhouse gas forcing in a non-flux-adjusted coupled climate codel, *J. Clim.*, *14*, 3102, doi:10.1175/1520-0442.

Vellinga, M., and P. Wu (2004), Low-latitude freshwater influence on centennial variability of the Atlantic thermohaline circulation, *J. Clim.*, *17*, 4498–4511.

Yeager, S. G., and W. G. Large (2004), Late-winter generation of spiciness on subducted isopycnals, *J. Phys. Oceanogr.*, *34*, 1528, doi:10.1175/1520-0485.

A. Laurian, A. Lazar, G. Reverdin, K. Rodgers, and P. Terray, Laboratoire d'Océanographie et du Climat: Expérimentation et Approche Numérique, Institut Pierre Simon Laplace, 4, place Jussieu, F-75252 Paris Cedex 05, France. (audine.laurian@lodyc.jussieu.fr)